

Selective Inhibition of Carboxylesterases by Isatins, Indole-2,3-diones

Janice L. Hyatt,[†] Teri Moak,[‡] M. Jason Hatfield,[†] Lyudmila Tsurkan,[†] Carol C. Edwards,[†] Monika Wierdl,[†] Mary K. Danks,[†] Randy M. Wadkins,[‡] and Philip M. Potter^{*†}

Department of Molecular Pharmacology, St. Jude Children's Research Hospital, Memphis, Tennessee 38105, Department of Chemistry and Biochemistry, University of Mississippi, University, Mississippi 38677

Received December 22, 2006

Carboxylesterases (CE) are ubiquitous enzymes thought to be responsible for the metabolism and detoxification of xenobiotics. Numerous clinically used drugs including Demerol, lidocaine, capecitabine, and CPT-11 are hydrolyzed by these enzymes. Hence, the identification and application of selective CE inhibitors may prove useful in modulating the metabolism of esterified drugs *in vivo*. Having recently identified benzil (diphenylethane-1,2-dione) as a potent selective inhibitor of CEs, we sought to evaluate the inhibitory activity of related 1,2-diones toward these enzymes. Biochemical assays and kinetic studies demonstrated that isatins (indole-2,3-diones), containing hydrophobic groups attached at a variety of positions within these molecules, could act as potent, specific CE inhibitors. Interestingly, the inhibitory potency of the isatin compounds was related to their hydrophobicity, such that compounds with *clogP* values of <1.25 were ineffective at enzyme inhibition. Conversely, analogs demonstrating *clogP* values >5 routinely yielded K_i values in the nM range. Furthermore, excellent 3D QSAR correlates were obtained for two human CEs, hCE1 and hiCE. While the isatin analogues were generally less effective at CE inhibition than the benzils, the former may represent valid lead compounds for the development of inhibitors for use in modulating drug metabolism *in vivo*.

Introduction

Carboxylesterases (CE^a) have been postulated as general detoxification enzymes¹ responsible for the hydrolysis of carboxyl esters to the corresponding alcohol and carboxylic acid. In mammals, they tend to be expressed in tissues likely to be exposed to xenobiotics, including the liver, lung, small intestine, kidney, and so on. CEs also hydrolyze numerous clinically useful drugs such as Demerol and lidocaine, the anticancer agents capecitabine and CPT-11 (irinotecan, 7-ethyl-10-[4-(1-piperidino)-1-piperidino]carbonyloxycamptothecin), as well as the narcotics cocaine and heroin.^{1–4} Because these enzymes significantly influence drug biodistribution and half-life, we recently screened for compounds that might inhibit CEs, with the goal of developing these inhibitors for use *in vivo*. If successful, these inhibitors might be efficacious in prolonging the bioactivity of agents that are inactivated by CEs or, conversely, may reduce the toxicity of compounds that are activated by these enzymes.

Until recently, the identification of stable, potent, selective inhibitors of CEs had remained elusive. This was due, in part, to the considerable homology among CEs and other esterases, including acetylcholinesterase (AChE). While trifluoromethyl

ketones (Figure 1) have been proposed as selective CE inhibitors, these compounds are hygroscopic, hydrolyzed by water to yield inactive components, and inhibit AChE.^{5,6} While potentially useful in *in vitro* biochemical studies, it is unlikely that these agents would be employed in preclinical or clinical applications. Several organophosphate-based compounds that have been described as irreversible, selective inhibitors of CEs have been developed (Bomin-1, -2, and -3; Figure 1); however, these agents also inhibit butyrylcholinesterase (BChE), and there are no published reports of these inhibitors being used in biological systems.

Our previous studies to identify selective CE inhibitors, based upon Telik's target-related affinity profiling technology,^{7–9} identified benzil (diphenylethane-1,2-dione; Figure 1) as a prototypic member of a class of diones that could inhibit these enzymes.¹⁰ In addition, heterocyclic analogues of benzil have also been demonstrated to be effective inhibitors of these proteins.¹¹ None of these dione-based inhibitors demonstrated any effect on human AChE or BChE. Furthermore, benzil and its analogues are stable under normal physiological conditions and are nontoxic.

Both biochemical and QSAR (quantitative structure–activity relationship) analyses of the benzil-based compounds indicated that the presence of aromatic moieties adjacent to the dione structure improved the potency of CE inhibition. In addition, we determined that both substrate hydrolysis and CE inhibition by different agents was dependent upon the size of the target molecule.^{10,12} Therefore, we attempted to identify small dione-containing compounds that might inhibit a wide spectrum of CEs. We reasoned that incorporating the dione chemotype within fused aromatic rings may reduce the size of the inhibitor and would likely retain the aromatic character of the molecule necessary for CE inhibition. Therefore, we hypothesized that their inhibitory activity toward a panel of CEs would be improved. Consequently, we searched databases of commercially available compounds for molecules that contained the dione

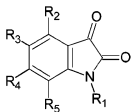
* To whom correspondence should be addressed. Dr. Philip M. Potter, Department of Molecular Pharmacology, St. Jude Children's Research Hospital, 332 N. Lauderdale, Memphis, TN 38105-2794. Tel.: 901-495-3440. Fax: 901-521-1668. E-mail: phil.potter@stjude.org.

[†] St. Jude Children's Research Hospital.

[‡] University of Mississippi.

^a Abbreviations: AChE, acetylcholinesterase; BChE, butyrylcholinesterase; benzil, diphenylethane-1,2-dione; BNPP, bis(4-nitrophenyl) phosphate; CE, carboxylesterase; *clogP*, calculated logP value; CPT-11, irinotecan, 7-ethyl-10-[4-(1-piperidino)-1-piperidino]carbonyloxycamptothecin; DMSO, dimethyl sulfoxide; hCE1, human carboxylesterase 1; hiCE, human intestinal carboxylesterase; *i*, fractional inhibition; isatin, 1*H*-indole-2,3-dione; K_i , inhibition constant; MAO, monoamine oxidase; *o*-NPA, *o*-nitrophenyl acetate; q^2 , cross correlation coefficients; QSAR, quantitative structure–activity relationship; rCE, rabbit liver carboxylesterase; Spearman *r*, Spearman rank correlation coefficient.

Table 1. Structure of the Isatins Used in This Article



R = H unless otherwise indicated

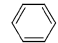
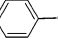
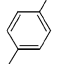
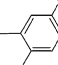
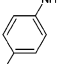
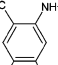
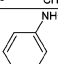
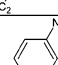
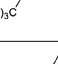
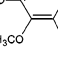
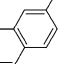
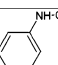
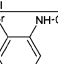
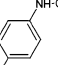
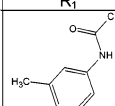
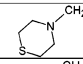
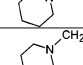
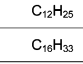
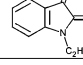
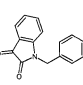
ID	Name	R ₁	R ₂	R ₃	R ₄	R ₅
1	1 <i>H</i> -indole-2,3-dione					
2	1-Methyl-1 <i>H</i> -indole-2,3-dione	CH ₃				
3	1-Hydroxymethyl-1 <i>H</i> -indole-2,3-dione	CH ₂ OH				
4	1-Chloro-1 <i>H</i> -indole-2,3-dione	Cl				
5	1-(2-Bromoethyl)-1 <i>H</i> -indole-2,3-dione	C ₂ H ₄ Br				
6	1-(2-Iodoethyl)-1 <i>H</i> -indole-2,3-dione	C ₂ H ₄ I				
7	1-Acetyl-1 <i>H</i> -indole-2,3-dione	COCH ₃				
8	1-(Chloroacetyl)-1 <i>H</i> -indole-2,3-dione	COCH ₂ Cl				
9	1-Propionyl-1 <i>H</i> -indole-2,3-dione	COC ₂ H ₅				
10	1-Butyryl-1 <i>H</i> -indole-2,3-dione	COC ₃ H ₇				
11	(2,3-Dioxo-2,3-dihydro-1 <i>H</i> -indol-1-yl) acetic acid	CH ₂ COOH				
12	2-(2,3-Dioxo-2,3-dihydro-1 <i>H</i> -indol-1-yl) acetamide	CH ₂ CONH ₂				
13	1-Phenyl-1 <i>H</i> -indole-2,3-dione					
14	1-Benzyl-1 <i>H</i> -indole-2,3-dione					
15	1-(4-Chlorobenzyl)-1 <i>H</i> -indole-2,3-dione					
16	1-(3,4-Dichlorobenzyl)-1 <i>H</i> -indole-2,3-dione					
17	1-((4-Methylphenyl)amino)methyl)-1 <i>H</i> -indole-2,3-dione					
18	1-(((2,4,5-Trimethylphenyl)amino)methyl)-1 <i>H</i> -indole-2,3-dione					
19	1-(((4-Ethylphenyl)amino)methyl)-1 <i>H</i> -indole-2,3-dione					
20	1-(((4-tert-Butylphenyl)amino)methyl)-1 <i>H</i> -indole-2,3-dione					
21	1-(((3,4,5-Trimethoxyphenyl)amino)methyl)-1 <i>H</i> -indole-2,3-dione					
22	1-((2-Naphthyl)amino)methyl)-1 <i>H</i> -indole-2,3-dione					
23	1-(((4-Chlorophenyl)amino)methyl)-1 <i>H</i> -indole-2,3-dione					
24	1-(((2-Bromophenyl)amino)methyl)-1 <i>H</i> -indole-2,3-dione					
25	1-(((4-Bromophenyl)amino)methyl)-1 <i>H</i> -indole-2,3-dione					
26	2-(2,3-Dioxo-2,3-dihydro-1 <i>H</i> -indol-1-yl)- <i>N</i> -(4-hydroxyphenyl) acetamide					
27	2-(2,3-Dioxo-2,3-dihydro-1 <i>H</i> -indol-1-yl)- <i>N</i> -(3-methylphenyl) acetamide					
28	4-Ethyl-1 <i>H</i> -indole-2,3-dione		C ₂ H ₅			
29	4-Chloro-1 <i>H</i> -indole-2,3-dione		Cl			
30	5-Methyl-1 <i>H</i> -indole-2,3-dione			CH ₃		
31	5-Methoxy-1 <i>H</i> -indole-2,3-dione			CH ₃ O		
32	5-Fluoro-1 <i>H</i> -indole-2,3-dione			F		
33	5-Chloro-1 <i>H</i> -indole-2,3-dione			Cl		
34	5-Bromo-1 <i>H</i> -indole-2,3-dione			Br		
35	5-Iodo-1 <i>H</i> -indole-2,3-dione			I		
36	5-(Trifluoromethoxy)-1 <i>H</i> -indole-2,3-dione			CF ₃ O		
37	5-Nitro-1 <i>H</i> -indole-2,3-dione			NO ₂		
38	5-Bromo-1-(2-methylprop-2-en-1-yl)-1 <i>H</i> -indole-2,3-dione	CH ₂ (C=CH ₂)CH ₃		Br		
39	6-Ethyl-1 <i>H</i> -indole-2,3-dione				C ₂ H ₅	
40	6-Chloro-1 <i>H</i> -indole-2,3-dione				Cl	
41	7-Methyl-1 <i>H</i> -indole-2,3-dione					CH ₃
42	7-Fluoro-1 <i>H</i> -indole-2,3-dione					F
43	7-Chloro-1 <i>H</i> -indole-2,3-dione					Cl
44	7-Methoxy-1 <i>H</i> -indole-2,3-dione					CH ₃ O
45	7-(Trifluoromethyl)-1 <i>H</i> -indole-2,3-dione					CF ₃
46	1 <i>H</i> -indole-2,3-dione -7-carboxylic acid					COOH
47	4,7-Methyl-1 <i>H</i> -indole-2,3-dione		CH ₃			CH ₃
48	5,7-Methyl-1 <i>H</i> -indole-2,3-dione			CH ₃		CH ₃
49	4,5-Dichloro-1 <i>H</i> -indole-2,3-dione		Cl	Cl		
50	4,6-Dichloro-1 <i>H</i> -indole-2,3-dione		Cl		Cl	
51	4,7-Dichloro-1 <i>H</i> -indole-2,3-dione		Cl			Cl
52	5,6-Dichloro-1 <i>H</i> -indole-2,3-dione			Cl	Cl	
53	5,7-Dichloro-1 <i>H</i> -indole-2,3-dione			Cl		Cl
54	6,7-Dichloro-1 <i>H</i> -indole-2,3-dione				Cl	Cl
55	4-Chloro-7-methyl-1 <i>H</i> -indole-2,3-dione		Cl			CH ₃
56	5-Chloro-7-methyl-1 <i>H</i> -indole-2,3-dione			Cl		CH ₃
57	6-Chloro-7-methyl-1 <i>H</i> -indole-2,3-dione				Cl	CH ₃
58	6-Bromo-5-methyl-1 <i>H</i> -indole-2,3-dione			CH ₃	Br	
59	1-(Thiomorpholin-4-ylmethyl)-1 <i>H</i> -indole-2,3-dione					
60	1-(Piperidin-1-ylmethyl)-1 <i>H</i> -indole-2,3-dione					
61	1-(Morpholin-4-ylmethyl)-1 <i>H</i> -indole-2,3-dione					
62	1-Dodecyl-1 <i>H</i> -indole-2,3-dione	C ₁₂ H ₂₅				
63	1-Hexadecyl-1 <i>H</i> -indole-2,3-dione	C ₁₆ H ₃₃				
64	1,1'-Ethane-1,2-diybis(1 <i>H</i> -indole-2,3-dione)					
65	1-(4-{4[(2,3-Dioxo-2,3-dihydro-1 <i>H</i> -indol-1-yl)methyl]benzyl}benzyl)-1 <i>H</i> -indole-2,3-dione					

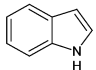
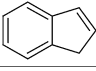
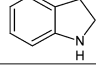
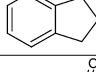
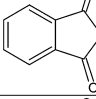
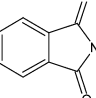
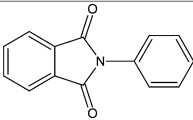
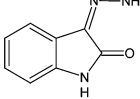
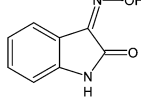
Table 2. K_i Values for the Isatins with Mammalian Esterases

ID	$K_i \pm SE$ (μM) for indicated enzyme					clogP
	hiCE	hCE1	rCE	AChE	BChE	
1	>100	>100	>100	>100	>100	0.87
2	38.2 \pm 4.0	5.38 \pm 0.41	>100	>100	>100	0.65
3	34.5 \pm 1.0	>100	>100	>100	>100	0.53
4	29.2 \pm 10.3	22.8 \pm 4.1	4.83 \pm 0.5	>100	>100	1.30
5	1.58 \pm 0.05	0.29 \pm 0.03	5.15 \pm 0.33	>100	28.1 \pm 6.4	1.64
6	0.74 \pm 0.10	0.13 \pm 0.01	2.15 \pm 0.33	>100	>100	1.97
7	>100	36.0 \pm 5.3	>100	>100	>100	0.41
8	>100	>100	>100	>100	>100	0.69
9	>100	17.5 \pm 1.5	>100	>100	>100	1.04
10	68.2 \pm 16.6	7.69 \pm 0.93	27.4 \pm 13.8	>100	>100	1.69
11	>100	>100	>100	>100	>100	-0.02
12	>100	>100	>100	>100	>100	-1.39
13	0.95 \pm 0.12	0.023 \pm 0.002	0.61 \pm 0.10	>100	68.8 \pm 14.4	1.66
14	0.87 \pm 0.05	1.70 \pm 0.36	19.0 \pm 5.7	>100	>100	1.89
15	0.032 \pm 0.003	0.025 \pm 0.003	0.75 \pm 0.13	>100	21.9 \pm 6.9	2.68
16	0.067 \pm 0.005	0.031 \pm 0.001	0.065 \pm 0.003	48.2 \pm 17.8	12.6 \pm 1.8	3.23
17	1.08 \pm 0.09	2.65 \pm 0.27	7.40 \pm 2.45	>100	18.1 \pm 0.5	2.76
18	2.88 \pm 0.04	1.62 \pm 0.10	8.29 \pm 0.22	>100	2.39 \pm 0.27	3.98
19	0.41 \pm 0.06	1.88 \pm 0.17	4.04 \pm 0.32	>100	12.3 \pm 0.3	4.06
20	0.61 \pm 0.07	1.42 \pm 0.24	16.7 \pm 3.4	>100	18.9 \pm 8.2	4.56
21	2.69 \pm 0.15	19.5 \pm 5.0	>100	>100	>100	3.01
22	0.11 \pm 0.03	>100	>100	>100	>100	2.59
23	0.20 \pm 0.01	0.61 \pm 0.08	1.12 \pm 0.42	>100	>100	3.62
24	0.047 \pm 0.002	36.0 \pm 5.3	1.15 \pm 0.23	>100	7.40 \pm 2.1	2.99
25	0.17 \pm 0.01	0.58 \pm 0.13	1.25 \pm 0.14	>100	>100	2.95
26	>100	>100	>100	>100	>100	0.98
27	5.51 \pm 0.37	4.35 \pm 0.32	4.90 \pm 0.85	>100	21.0 \pm 5.2	1.93
28	37.9 \pm 9.7	>100	34.9 \pm 3.9	>100	>100	1.25
29	7.77 \pm 0.71	8.25 \pm 0.88	3.29 \pm 0.15	>100	>100	1.34
30	>100	>100	26.2 \pm 3.5	>100	>100	1.23
31	>100	>100	26.7 \pm 3.5	>100	>100	1.17
32	>100	>100	>100	>100	>100	0.83
33	14.9 \pm 4.0	1.22 \pm 0.62	4.37 \pm 2.64	>100	>100	1.57
34	13.3 \pm 2.3	31.7 \pm 6.6	1.32 \pm 0.45	>100	>100	1.60
35	22.8 \pm 3.6	26.9 \pm 8.4	1.16 \pm 0.09	>100	>100	1.95
36	7.94 \pm 1.54	16.5 \pm 10.0	0.36 \pm 0.12	>100	>100	1.56
37	>100	>100	6.43 \pm 0.15	>100	>100	0.75
38	0.28 \pm 0.02	0.066 \pm 0.003	0.13 \pm 0.01	>100	>100	1.89
39	>100	>100	29.5 \pm 6.0	>100	>100	1.84
40	29.7 \pm 12.1	53.9 \pm 7.7	14.6 \pm 0.9	>100	>100	1.57
41	>100	>100	>100	>100	>100	0.74
42	>100	>100	>100	>100	>100	0.78
43	9.55 \pm 4.71	11.4 \pm 0.6	4.51 \pm 0.19	>100	30.6 \pm 12.2	1.38
44	>100	>100	16.1 \pm 9.4	>100	>100	0.84
45	33.4 \pm 6.0	13.1 \pm 1.2	2.15 \pm 0.33	>100	>100	1.30
46	>100	>100	>100	>100	>100	1.07
47	30.8 \pm 8.2	>100	>100	>100	>100	0.61
48	84.6 \pm 19.8	>100	30.5 \pm 1.8	>100	>100	1.12
49	2.56 \pm 0.18	3.02 \pm 0.25	0.41 \pm 0.02	>100	>100	1.90
50	0.62 \pm 0.03	0.89 \pm 0.06	0.53 \pm 0.01	>100	>100	2.02
51	0.65 \pm 0.05	0.59 \pm 0.05	0.41 \pm 0.04	>100	>100	1.85
52	16.6 \pm 2.8	21.0 \pm 2.0	0.49 \pm 0.03	>100	>100	2.18
53	4.08 \pm 0.37	3.52 \pm 0.33	0.76 \pm 0.03	>100	>100	2.06
54	21.8 \pm 2.6	9.40 \pm 0.7	1.42 \pm 0.11	>100	>100	1.94
55	17.2 \pm 1.6	5.53 \pm 0.23	16.7 \pm 4.1	>100	>100	1.33
56	21.8 \pm 2.0	34.1 \pm 10.7	14.1 \pm 2.1	>100	>100	1.67
57	53.5 \pm 20.6	55.3 \pm 19.1	12.1 \pm 3.3	>100	>100	1.30
58	7.41 \pm 0.88	16.5 \pm 2.0	0.42 \pm 0.07	>100	56.5 \pm 17.8	1.83
59	22.2 \pm 8.1	>100	>100	>100	98.9 \pm 3.8	0.75
60	27.4 \pm 11.3	>100	>100	>100	>100	1.24
61	22.5 \pm 4.3	>100	>100	>100	>100	0.25
62	0.008 \pm 0.001	0.010 \pm 0.002	0.088 \pm 0.006	>100	>100	6.27
63	0.011 \pm 0.001	0.016 \pm 0.001	>100	>100	>100	6.58
64	1.54 \pm 0.08	1.56 \pm 0.31	10.5 \pm 1.2	>100	6.71 \pm 1.78	1.40
65	0.010 \pm 0.002	0.008 \pm 0.002	0.006 \pm 0.002	3.28 \pm 0.73	>100	5.11

increase the potency of CE inhibition.^{10,11} Based upon this information, we searched for molecules that contained a dione group located proximal to an aromatic ring. These criteria identified isatin (Figure 1) as a potential target molecule. Because numerous analogues of isatin were available, we assessed the ability of these compounds to inhibit metabolism of the general esterase substrate *o*-NPA by CEs.

K_i Values for Isatin Analogues with Mammalian CEs. We identified 65 commercially available isatin analogues, which included 33 with *N*-substitutions, 2 with substituents at the 4-position, 8 at the 5-position, 2 at the 6-position, and 6 at the 7-position. Thirteen analogues contained different chemical groups at multiple positions within the benzene ring. The structures of these compounds are indicated in Table 1. We then

Table 3. Control Compounds Assessed for CE Inhibition^a

ID	Name	Structure
66	1 <i>H</i> -Indole	
67	1 <i>H</i> -Indene	
68	Indoline	
69	Indane	
70	1 <i>H</i> -Indene-1,3(2 <i>H</i>)-dione	
71	1 <i>H</i> -isoindole-1,3(2 <i>H</i>)-dione	
72	2-Phenyl-1 <i>H</i> -isoindole-1,3(2 <i>H</i>)-dione	
73	(3 <i>Z</i>)-1 <i>H</i> -Indole-2,3-dione 3-hydrazone	
74	(3 <i>Z</i>)-1 <i>H</i> -Indole-2,3-dione 3-oxime	

^a None of these isatin analogues demonstrated any enzyme inhibition at concentrations up to 100 μM .

determined the K_i values for these compounds with two human CEs, hiCE and hCE1, and rCE, using o-NPA as a substrate. The K_i values for the inhibition of the mammalian CEs are displayed in Table 2.

A wide variation in the K_i values were observed with the isatin analogues ranging from $>100 \mu\text{M}$ (no enzyme inhibition) to as low as 6 nM (compound **65** with rCE). Generally, compounds that inhibited one CE also inhibited the other two enzymes, however, there were exceptions. For example, the *N*-naphthylamino derivative (**22**) was a potent inhibitor of hiCE ($K_i = 110 \text{ nM}$), but demonstrated no activity against hCE1 or rCE. Similarly, compound **37** was a relatively good inhibitor of rCE ($K_i = 6.43 \mu\text{M}$), but demonstrated no activity toward the two human proteins. However, it should be noted that for the vast majority of the isatin analogues, inhibition demonstrated by most of the compounds was common among the three mammalian CEs.

Analysis of CE inhibition was also undertaken using a series of analogues demonstrating structural homology to isatin (Table 3). None of these compounds inhibited the mammalian CEs at concentrations up to 100 μM (data not shown). Because these analogues lack the 1,2-dione moiety, these studies suggest that this function is essential for CE inhibition.

Inhibition of Human Acetyl- and Butyrylcholinesterase. To assess the specificity of CE enzyme inhibition, we assayed the ability of these compounds to inhibit human AChE or BChE. As indicated in Table 2, inhibition of AChE was only observed with two compounds, **16** and **65**, with K_i values of 48.2 μM and 3.28 μM , respectively. More commonly, however, BChE

Table 4. Correlation Parameters for the ClogP Values of the Inhibitors with the Observed K_i Values for the Mammalian CEs

parameter	enzyme		
	hiCE	hCE1	rCE
r^2 (linear regression)	0.635	0.388	0.211
Spearman r	-0.809	-0.518	-0.465
<i>P</i> value for Spearman	<0.0001	0.0004	0.0011

was inhibited by these isatin analogues (Table 2). Fourteen compounds demonstrated inhibition of human BChE; however, the majority of these were relatively weak inhibitors, with K_i values typically in the 20–60 μM range. In contrast, several molecules were relatively potent at inhibiting this enzyme. For example, **24** and **64** had K_i values of less than 10 μM (7.40 μM and 6.71 μM , respectively). However, because the exact function and endogenous substrate of BChE is unclear and individuals who demonstrate reduced levels or complete loss of this protein are apparently healthy,^{32–34} it is unlikely that the clinical use of these inhibitors would yield effects related to inhibition of this protein.

Correlation between K_i Values and logP. In general, for the isatin analogues, there was a correlation between the calculated logP and the K_i values for the inhibition of CEs. For example, compounds with predicted logP values of less than 1.25 (compounds **1**, **3**, **7–9**, **11**, **12**, **25**, **29–31**, **36**, **40**, **41**, **43**, **45–47**, and **58–60**) were poor inhibitors of o-NPA hydrolysis. Interestingly, regression analysis of the clogP versus the K_i constants for the different enzymes did yield moderate linear correlation coefficients, (r^2 ranging from 0.211 to 0.635; Table 4; Figure 2).

However, because any correlation between the K_i and the logP values was unlikely to be linear, we performed nonparametric statistical analysis. The Spearman *r* values, comparing the observed K_i values with the calculated logP of the inhibitors, were therefore calculated. These analyses yielded Spearman *r* values of -0.809, -0.518, and -0.465, for hiCE, hCE1, and rCE, respectively (Table 4). Because a Spearman *r* value of -1 indicates a perfect negative correlation and 0 indicates no correlation, these analyses suggest that there is a strong association between these two parameters. The *P* values associated with the statistical analyses of these data sets ranged from <0.0001 to 0.0011 (Table 4), indicating that the K_i values were highly correlated with the clogP of the inhibitor.

Assessment of the Mode of Carboxylesterase Inhibition by the Isatin Analogues. To determine whether the inhibition of CEs was reversible, we preincubated selected inhibitors (compounds **13**, **16**, **23**, and **38**) with the enzymes on ice for 1 h and then assessed enzyme activity. As indicated in Figure 3, after dilution of the inhibitor from the reactions, all of the enzymes retained hydrolytic activity. Irreversible inhibition of all of the CEs was only seen with the control organophosphate BNPP. Because none of the isatin analogues analyzed irreversibly inhibit the enzymes, it is likely that the compounds interact with the catalytic amino acids in a fashion similar to benzil.¹⁰

3D-QSAR Pseudoreceptor Models of Isatin-Mediated Inhibition of CEs. Using Quasar software, 3D pseudoreceptor models were generated from the inhibition datasets for the isatin analogues and enzyme-ligand binding sites. These models for the human CEs good q^2 values with values of 0.767 and 0.729 for hiCE and hCE1, respectively (Table 5). In addition, r^2 correlates for the observed versus predicted K_i values were >0.79 , demonstrating the validity of the 3D-QSAR analyses (Figure 4). We derived pseudoreceptor site models for hiCE and hCE1 from these analyses, and these are depicted in Figure 5.

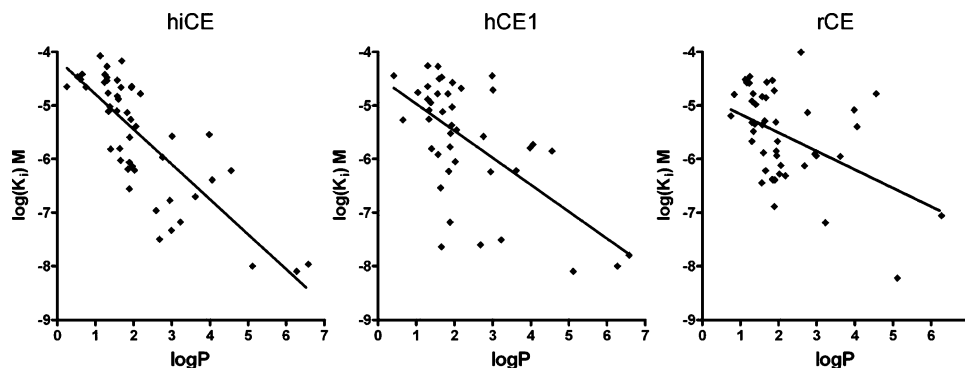


Figure 2. Graphs demonstrating the correlation between the K_i values for enzyme inhibition and the calculated $\log P$ constants for the isatin analogues for three mammalian CEs. The r^2 values for the line fits were 0.64, 0.39, and 0.21 for hiCE, hCE1, and rCE, respectively.

As can be seen, a distribution of anionic (red) and cationic (blue) regions within the pseudoreceptor site were required for the accurate fitting of the data set to the 3D models. This is consistent with previous models that we have generated by this method for benzene sulfonamide,³⁵ benzil,¹⁰ and trifluoroketone³⁶ inhibitors of CEs. The isatin analogue **14** is positioned within the model in an orientation similar to that of benzil in previous studies. While it is impossible to assign an orientation to a QSAR model, mapping of the charge distribution of the model to the corresponding amino acid types in the CE crystal structure¹⁰ suggests that the orientation shown in Figure 5 is such that the bottom of the figure represents the region of active site containing the catalytic amino residues. The relatively uncharged region toward the top likely represents the active site gorge, which is lined with hydrophobic residues in these enzymes. This model indicates that the indole ring system of **14** interacts with a highly polarized environment in the gorge, whereas the upper ring (the benzyl moiety in **14**) is located in a more hydrophobic region of the protein, as indicated by the absence of charged spheres in Figure 5. This is particularly apparent for the 3D-pseudoreceptor site model of hiCE.

However, for rCE, both the r^2 value for the observed versus predicted K_i values and the q^2 were poor (0.297 and 0.309, respectively). Because the latter value is below that required for acceptable inhibitor design (0.4),³⁷ it is unlikely that the rCE QSAR model would be suitable for further improvement in the potency of the isatin analogues. We believe that the poor correlations observed with rCE are due to the relatively small range of K_i values over the 10^{-5} – 10^{-7} M inhibitor concentrations. We did not generate a 3D-QSAR pseudoreceptor site model for rCE, because the validity of such a model, in light of the r^2 and q^2 values, was unclear.

Molecular Modeling of Isatin Inhibitors. The pseudoreceptor site models are generated in the absence of information from the protein and represent the field in which the inhibitor interacts with the amino acid residues. In an attempt to directly determine how the isatins associate with the catalytic amino acids in the CEs, we performed molecular modeling using ICM-Pro software. Four analogues were chosen for analysis, compounds **1**, **14**, **32**, and **38**, because they represent analogs that demonstrate no inhibition (**1** and **32**) and good inhibition (**14** and **38**) with the different CEs. After docking into the active site of hCE1 (using the coordinates of the X-ray crystal structure of this protein), the distances between catalytic serine and the inhibitor atoms were measured. While we observed no significant differences between compounds that could and could not inhibit the enzymes, all of the isatins localized such that at least one of the carbonyl carbon atoms was within 3.6 Å of the serine O γ atom (Figure 6). This was comparable to the distance (3.4

Å) observed between the corresponding atoms following docking of the CE substrate o-NPA into the hCE1 active site. Because nucleophilic attack by the serine O γ atom toward the carbonyl carbon in the ester group is the initial step in substrate hydrolysis,³⁸ it is likely that a similar mechanism may occur with isatin-mediated inhibition of CEs (Figure 7).

However, it should be noted that compounds **1** and **32** adopted a similar conformation within the active site gorge of hCE1. As can be seen in Figure 6 (panels A and C), isatin (**1**) and 5-fluoroisatin (**32**) could be overlaid in an almost identical position (Figure 6E), with both indole carbonyl carbon atoms approximately 3.6 Å from the serine O γ atom. In contrast, the compounds that effectively inhibited hCE1 (**14** and **38**) localized in a different conformation to **1** and **32**, with at least one of the carbonyl carbon atoms within 3.5 Å of the oxygen nucleophile. Whether these differences account for enzyme inhibition is unclear, but these studies clearly demonstrate that the isatin analogues can juxtapose to the catalytic amino acids in hCE1, at distances where interactions with active site serine are likely to occur.

Discussion

Until recently, the identification of selective CE inhibitors has proven problematic. This is, in part, due to the fact that these enzymes demonstrate considerable amino acid and structural homology to AChE. Hence, compounds that are marketed as general esterase inhibitors (e.g., BNPP) inhibit many different enzymes, including CEs, AChE, and BChE. Recently, we identified benzil as a selective CE inhibitor¹⁰ and demonstrated that the 1,2-dione domain was crucial for enzyme inhibition. Subsequently, we observed that the aromaticity of the ring domains was an important factor in the biological activity of these compounds.¹¹ Therefore, using this information, we searched the chemical databases for molecules that contained a 1,2-dione moiety within an aromatic ring structure. This identified isatin as a potential CE inhibitor. However, biochemical studies using this compound demonstrated no inhibition of the mammalian CEs when using o-NPA as a substrate (Table 2). In contrast, analogues containing hydrophobic substitutions, essentially at any position within the molecule (e.g., *N*-phenylisatin (**13**), 5-iodoisatin (**35**), 4,7-dichloroisatin (**51**)), were all potent inhibitors of CEs.

As indicated by the control compounds that we assayed (**66**–**74**), for a molecule to be an effective CE inhibitor it was necessary to contain the dione moiety in the 1,2-configuration. Additionally, we observed that compounds that were more lipophilic were better inhibitors (Table 2), with good correlations between inhibitor potency and the $\log P$ of the molecule (Figure 2 and Table 3). As the catalytic amino acid residues of CEs are

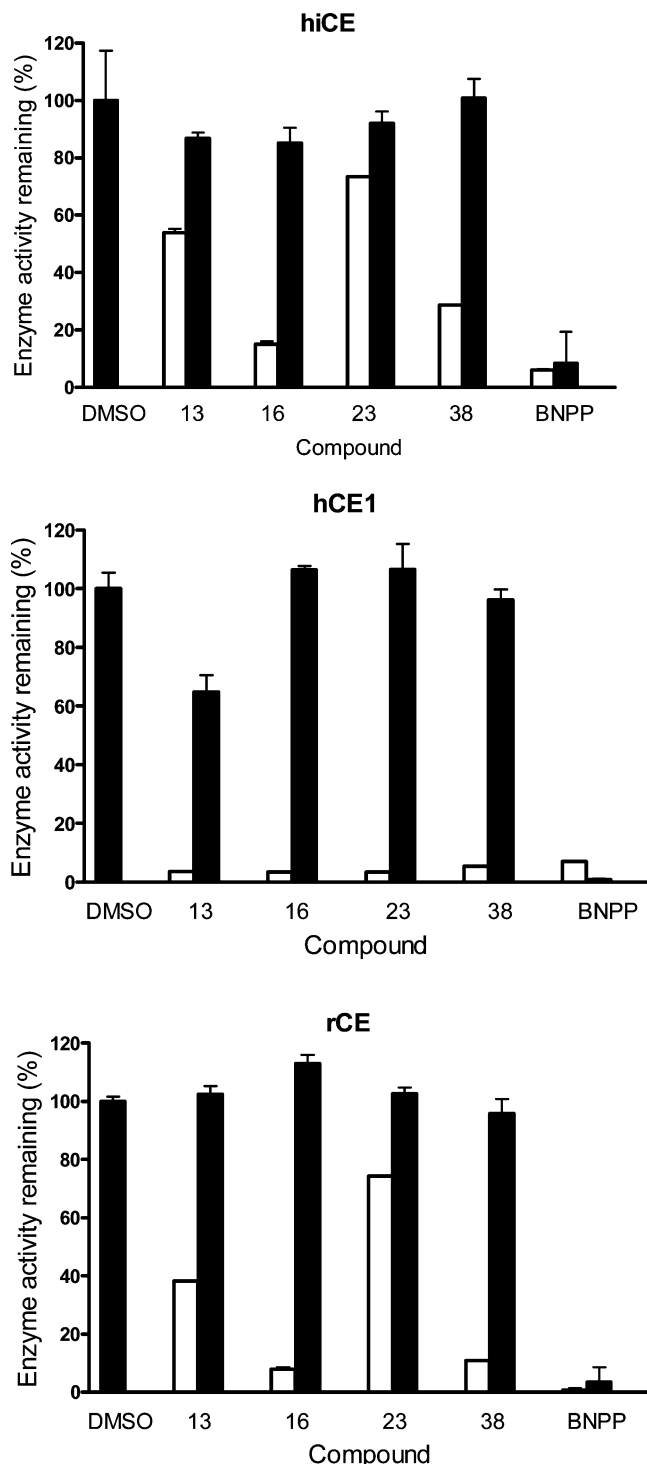


Figure 3. Graphs demonstrating the reversible inhibition of CEs by selected isatin analogues. Enzyme activity was determined after preincubation with the isatin analogues or BNPP for 1 h. The open bars represent results obtained from samples that have not been diluted, whereas the solid bars are data generated following a 500-fold dilution of the inhibitor (2 nM final concentration for the isatins).

buried at the bottom of deep hydrophobic gorges in these proteins,^{12,28,39,40} it is likely that this environment would be favorable for the localization of more lipophilic compounds. Hence, the binding affinity for more hydrophobic molecules (i.e., those with higher logP values) would be expected to be greater. The results that we have observed with the isatin analogues are consistent with this hypothesis.

The studies presented here, therefore, demonstrate the properties necessary for CE inhibition by these types of compounds.

Table 5. Correlation Coefficients for the Isatin CE QSAR Models

enzyme	observed versus predicted K_i values (r^2)	q^2	q^2/r^2
hiCE	0.810	0.767	1.05
hCE1	0.794	0.729	1.09
rCE	0.297	0.309	0.96

First, a 1,2-dione chemotype is required preferably within, or adjacent to, an aromatic moiety. Second, the logP of the inhibitor must be greater than 1.25. By comparison, benzil has a clogP of 3.02. Third, any substitution within the fused benzene ring of the isatin must be small enough such that it does not impede access of the inhibitor to the enzyme active site. For example, the K_i values for the inhibition of hCE1 by **34**, **35**, or **36** are considerably lower than those seen for rCE with the same compounds (Table 2). As we have previously demonstrated that the entrance to the active site gorge in hCE1 is considerably smaller than that seen in rCE,¹² it is likely that bulky Br, I, or CF_3O groups present within these inhibitors reduce the ability of these compounds to access the catalytic amino acids that are located at the base of the active site gorge. For smaller substitutions, the effect on the K_i was negligible, as exemplified by inhibitors **29** and **43** (4-chloro- and 7-chloroisatin, respectively), which had very similar K_i values for all of the CEs tested.

The 3D-QSAR models generated for hiCE and hCE1 (Figure 5) provided some insights as to why the hydrophobicity of the isatin analogues is an important factor in enzyme inhibition. The models demonstrate hydrophobic zones in the center of an otherwise highly polar region. Addition of a second aromatic group, such as a phenyl or benzyl ring within the isatin molecule, allows the inhibitor to interact with this hydrophobic area (note the absence of spheres around the benzyl ring in Figure 5). Such a zone would likely be formed by the side chains from one or more hydrophobic amino acids in the catalytic regions of the protein. Because the active site gorges of CEs are known to be lined with many residues containing aromatic rings (e.g., Phe, Tyr, His, Trp³⁸), it is likely that this hydrophobic domain represents an important factor in the interaction of the isatin analogues with the catalytic amino acids.

Molecular modeling studies using selected isatin analogues (**1**, **14**, **32**, and **38**) and the crystal structure of hCE1 did not identify any obvious reason for the lack of enzyme inhibition by compounds **1** and **32**. However, in these studies, the inhibitor was modeled within the active site gorge, and this approach would, therefore, eliminate any interactions that would occur with other domains of the protein. We have previously reported that the loops that form the entrance to the active site of hCE1 are highly ordered as compared to rCE^{28,40} and that these domains impact substrate metabolism.¹² Hence, while the modeling studies indicate that the inhibitors localize adjacent to the active site serine and likely interact with this amino acid, these models cannot explain the inhibitory action of the isatins.

The preincubation assays indicated that the inhibition of CEs by the isatin analogues was reversible. In addition, because the molecular modeling studies demonstrated that the carbonyl carbon atoms within the indole ring could localize within 3.5 Å of the catalytic nucleophile (the serine O γ atom; Figure 6), our results suggest that enzyme inhibition could be mediated by attack of either of these carbon atoms by the serine residue. Such a mechanism is depicted in Figure 7. Hence, following formation of the nucleophile by proton transfer through the histidine to the glutamic acid, the serine O γ atom would then attack the indole carbonyl group to generate the transient intermediate. However, for the reaction to continue, either the

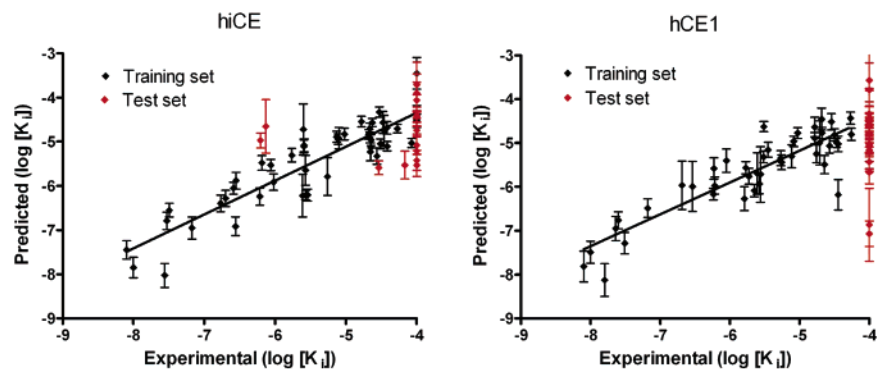


Figure 4. Graphs comparing the observed versus the predicted K_i values for the isatin analogues for hiCE and hCE1. Predicted data was obtained from the 3D-QSAR models obtained using Quasar software. In each case, the model was built using the training set (black diamonds) and then validated using the test set (red diamonds).

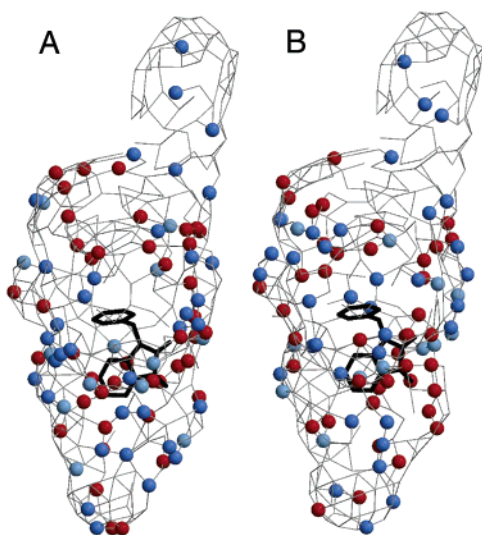


Figure 5. 3D-QSAR pseudoreceptor models obtained from the enzyme inhibition data for hiCE (panel A) and hCE1 (panel B) with the isatin analogues. The models are depicted as colored spheres on a hydrophobic gray grid. Hydrophobic areas are shown in gray, with dark blue spheres representing areas of positive charge ($+0.1e$) and light blue spheres corresponding to hydrogen bond donors. Orange spheres represent hydrogen bond acceptors and areas that are negatively charged ($-0.1e$) are displayed as orange-red spheres. In all cases, e corresponds to the charge of a proton. A representative isatin analogue (compound **14**) is drawn in black. The figure was constructed using Raster3D⁴⁵ and Molscript.⁴⁶

C–C or the C–N bond in the five-membered ring must be broken (Figure 7). This would then result in a covalent product bound to the serine residue that would likely irreversibly inhibit enzyme activity. A much more plausible scenario, based upon both the biochemical data and the molecular modeling studies, suggests that the formation of the initial intermediate is rapidly reversible, readily liberating free enzyme and inhibitor (Figure 7, lower panel). This mechanism is comparable to that observed for the inhibition of CEs by benzil.¹⁰

Because the indole moiety is present within a whole host of clinically used drugs (e.g., indomethacin, indoramin), it is likely that the isatin inhibitors will be better tolerated *in vivo* than the benzil derivatives. However, isatin and its analogues have also been demonstrated to be monoamine oxidase (MAO) inhibitors, with the most potent compounds containing substitutions at the 5-position within the indole ring.⁴¹ Additionally, the moieties appended at this position were small and demonstrated low hydrophobicity (e.g., OH, C_2H_5 , C_4H_9). This is in contrast to the majority of the potent CE inhibitors described here that

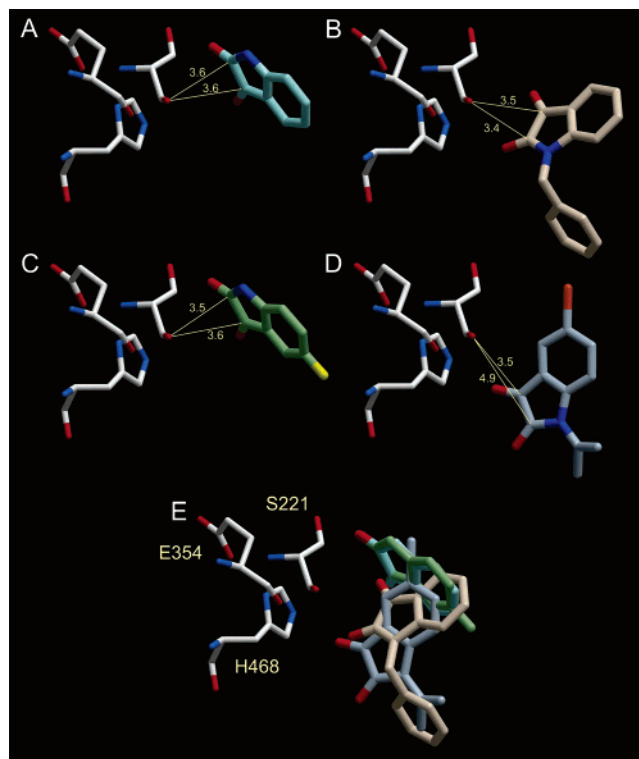


Figure 6. Molecular modeling of compounds **1** (panel A), **14** (panel B), **32** (panel C), and **38** (panel D) into the active site of hCE1. The three residues necessary for catalysis (S221, E354, and H468) are displayed, and the distances between the carbonyl carbon atoms and the serine O_γ are indicated in Angstroms. By comparison, the corresponding distance for the docking of the CE substrate *o*-NPA into the hCE1 active site is 3.4 Å. Panel E represents an overlay of all four of the isatin molecules using the coloring scheme in the previous panels. In all molecules, oxygen atoms are indicated in red, nitrogen atoms are depicted in blue, fluorine atoms are displayed in yellow, and bromine atoms are shown in orange.

contain large bulky hydrophobic substituents, mainly at the 1-position of the molecule (Tables 1 and 2). Furthermore, the IC_{50} values for the inhibition of either MAO A or MAO B by the isatin analogues were considerably higher (typically 1–20 μ M) than that seen for CE-mediated enzyme inhibition. By comparison, the most potent inhibitor that we have identified is compound **62** (1-dodecyl-1*H*-indole-2,3-dione), which demonstrates a K_i value of 8 nM for hiCE. Due to the increase in potency and the difference in the position of substitution within the molecule, we believe it is unlikely that inhibition of MAO would preclude the use of the isatins for CE inhibition *in vivo*.

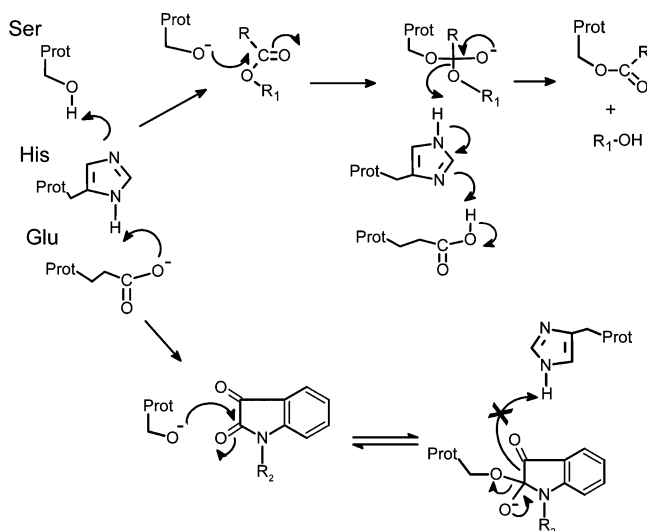


Figure 7. Proposed mechanism of interaction of isatin inhibitors with the catalytic amino acids in CEs. The upper panel depicts the mechanism of the initial stages of ester (RCOOR_1) hydrolysis by CEs with the serine (Ser), histidine (His), and glutamic acid (Glu). Nucleophilic attack by the serine O_γ on the carbonyl carbon results in a tetrahedral intermediate that decomposes to release the alcohol (R_1OH) and form a serine ester. In the lower panel, attack by the O_γ on one of the carbonyl carbons in an isatin analogue is displayed. However, for the reaction to continue, cleavage of the C–C bond in the pyrrole ring must occur. This is unlikely to happen in comparison to the cleavage of the ester C–O bond due to the enhanced strength of the former bond.

Recently, several isatin derivatives containing substitutions at the 5-position of the molecule have been demonstrated to be caspase 3/7 inhibitors.^{42–44} The most potent of these analogues contained a sulfonyl group attached to the nitrogen-containing ring as the substituent. In addition, 5-nitroisatin (**37**) was shown to be a good inhibitor of these caspases, with an IC_{50} value of $3 \mu\text{M}$.⁴⁴ We have not assayed the ability of the sulfonyl derivatives to inhibit CEs, however, compound **37** is not an inhibitor of the human CEs (Table 2). Clearly though, before development of any compounds for the *in vivo* inhibition of CEs (or caspases), the specificity of the isatins toward these classes of enzymes will need to be assessed.

Overall, the studies presented here demonstrate that isatin analogues, primarily those containing hydrophobic substituents, are potent, selective inhibitors of mammalian CEs. Their potency correlates with the clogP of the molecule, and 3D-QSAR models should allow for the design of more bioavailable, less toxic analogues. Such studies are currently underway.

Acknowledgment. This work was supported in part by NIH Grants CA76202, CA79763, CA98468, CA108775, and DA-18116, a Cancer Center Core Grant P30 CA 21765, and by the American Lebanese Syrian Associated Charities.

References

- Cashman, J.; Perroti, B.; Berkman, C.; Lin, J. Pharmacokinetics and molecular detoxification. *Environ. Health Perspect.* **1996**, *104*, 23–40.
- Kamendulis, L. M.; Brzezinski, M. R.; Pindel, E. V.; Bosron, W. F.; Dean, R. A. Metabolism of cocaine and heroin is catalyzed by the same human liver carboxylesterases. *J. Pharmacol. Exp. Ther.* **1996**, *279*, 713–717.
- Khanna, R.; Morton, C. L.; Danks, M. K.; Potter, P. M. Proficient metabolism of CPT-11 by a human intestinal carboxylesterase. *Cancer Res.* **2000**, *60*, 4725–4728.
- Redinbo, M. R.; Bencharit, S.; Potter, P. M. Human carboxylesterase 1: From drug metabolism to drug discovery. *Biochem. Soc. Trans.* **2003**, *31*, 620–624.
- Brodbeck, U.; Schweikert, K.; Gentinetta, R.; Rottenberg, M. Fluorinated aldehydes and ketones acting as quasi-substrate inhibitors of acetylcholinesterase. *Biochim. Biophys. Acta* **1979**, *567*, 357–369.
- Wheelock, C. E.; Colvin, M. E.; Uemura, I.; Olmstead, M. M.; Sanborn, J. R.; Nakagawa, Y.; Jones, A. D.; Hammock, B. D. Use of *ab initio* calculations to predict the biological potency of carboxylesterase inhibitors. *J. Med. Chem.* **2002**, *45*, 5576–5593.
- Beroza, P.; Villar, H. O.; Wick, M. M.; Martin, G. R. Chemoproteomics as a basis for post-genomic drug discovery. *Drug Discovery Today* **2002**, *7*, 807–814.
- Dixon, S. L.; Villar, H. O. Bioactive diversity and screening library selection via affinity fingerprinting. *J. Chem. Inf. Comput. Sci.* **1998**, *38*, 1192–1203.
- Kauvar, L. M.; Higgins, D. L.; Villar, H. O.; Sportsman, J. R.; Engqvist-Goldstein, A.; Bukar, R.; Bauer, K. E.; Dilley, H.; Rocke, D. M. Predicting ligand binding to proteins by affinity fingerprinting. *Chem. Biol.* **1995**, *2*, 107–118.
- Wadkins, R. M.; Hyatt, J. L.; Wei, X.; Yoon, K. J.; Wierdl, M.; Edwards, C. C.; Morton, C. L.; Obenauer, J. C.; Damodaran, K.; Beroza, P.; Danks, M. K.; Potter, P. M. Identification and characterization of novel benzil (diphenylethane-1,2-dione) analogues as inhibitors of mammalian carboxylesterases. *J. Med. Chem.* **2005**, *48*, 2905–2915.
- Hyatt, J. L.; Stacy, V.; Wadkins, R. M.; Yoon, K. J.; Wierdl, M.; Edwards, C. C.; Zeller, M.; Hunter, A. D.; Danks, M. K.; Crundwell, G.; Potter, P. M. Inhibition of carboxylesterases by benzil (diphenylethane-1,2-dione) and heterocyclic analogues is dependent upon the aromaticity of the ring and the flexibility of the dione moiety. *J. Med. Chem.* **2005**, *48*, 5543–5550.
- Wadkins, R. M.; Morton, C. L.; Weeks, J. K.; Oliver, L.; Wierdl, M.; Danks, M. K.; Potter, P. M. Structural constraints affect the metabolism of 7-ethyl-10-[4-(1-piperidino)-1-piperidino]carbonyloxycamptothecin (CPT-11) by carboxylesterases. *Mol. Pharmacol.* **2001**, *60*, 355–362.
- Munger, J. S.; Shi, G. P.; Mark, E. A.; Chin, D. T.; Gerard, C.; Chapman, H. A. A serine esterase released by human alveolar macrophages is closely related to liver microsomal carboxylesterases. *J. Biol. Chem.* **1991**, *266*, 18832–18838.
- Potter, P. M.; Pawlik, C. A.; Morton, C. L.; Naeve, C. W.; Danks, M. K. Isolation and partial characterization of a cDNA encoding a rabbit liver carboxylesterase that activates the prodrug Irinotecan, (CPT-11). *Cancer Res.* **1998**, *52*, 2646–2651.
- Morton, C. L.; Potter, P. M. Comparison of *Escherichia coli*, *Saccharomyces cerevisiae*, *Pichia pastoris*, *Spodoptera frugiperda* and COS7 cells for recombinant gene expression: Application to a rabbit liver carboxylesterase. *Mol. Biotechnol.* **2000**, *16*, 193–202.
- Schwer, H.; Langmann, T.; Daig, R.; Becker, A.; Aslanidis, C.; Schmitz, G. Molecular cloning and characterization of a novel putative carboxylesterase, present in human intestine and liver. *Biochem. Biophys. Res. Commun.* **1997**, *233*, 117–120.
- Beaufay, H.; Amar-Costesec, A.; Feytmans, E.; Thines-Sempoux, D.; Wibó, M.; Robbi, M.; Berthet, J. Analytical study of microsomes and isolated subcellular membranes from rat liver. I. Biochemical methods. *J. Cell Biol.* **1974**, *61*, 188–200.
- Doctor, B. P.; Toker, L.; Roth, E.; Silman, I. Microtiter assay for acetylcholinesterase. *Anal. Biochem.* **1987**, *166*, 399–403.
- Ellman, G. L.; Courtney, K. D.; Anders, V.; Featherstone, R. M. A new and rapid colorimetric determination of acetylcholinesterase activity. *Biochem. Pharmacol.* **1961**, *7*, 88–95.
- Webb, J. L. *Enzyme and Metabolic Inhibitors. Volume 1. General Principles of Inhibition*; Academic Press Inc.: New York, 1963.
- Akaike, H. In *Information theory and an extension of the maximum likelihood principle*, Second International Symposium on Information Theory, Budapest, 1973; Petrov, B. N., Csaki, F., Eds.; Akademiai Kiado: Budapest, 1973; pp 267–281.
- Akaike, H. A new look at the statistical model identification. *IEEE Trans. Autom. Control* **1974**, *AC-19*, 716–723.
- Stewart, J. J. MOPAC: A semiempirical molecular orbital program. *J. Comput.-Aided Mol. Des.* **1990**, *4*, 1–105.
- Vedani, A.; Dobler, M. Multidimensional QSAR: Moving, from three- to five-dimensional concepts. *Quant. Struct.-Act. Relat.* **2002**, *21*, 382–390.
- Vedani, A.; Dobler, M. 5D-QSAR: The key for simulating induced fit? *J. Med. Chem.* **2002**, *45*, 2139–2149.
- Vedani, A.; Dobler, M.; Lill, M. A. Combining, protein modeling, and 6D-QSAR simulating the binding of structurally diverse ligands to the estrogen receptor. *J. Med. Chem.* **2005**, *48*, 3700–3703.
- Jakalian, A.; Jack, D. B.; Bayly, C. I. Fast efficient generation of high-quality atomic charges. AM1-BCC model: II. Parameterization and validation. *J. Med. Chem.* **2002**, *23*, 1623–1641.

- (28) Bencharit, S.; Morton, C. L.; Hyatt, J. L.; Kuhn, P.; Danks, M. K.; Potter, P. M.; Redinbo, M. R. Crystal structure of human carboxylesterase 1 complexed with the Alzheimer's drug tacrine. From binding promiscuity to selective inhibition. *Chem. Biol.* **2003**, *10*, 341–349.
- (29) Chen, H.; Lyne, P. D.; Giordanetto, F.; Lovell, T.; Li, J. On evaluating molecular-docking methods for pose prediction and enrichment factors. *J. Chem. Inf. Model.* **2006**, *46*, 401–415.
- (30) Cavasotto, C. N.; Orry, A. J.; Abagyan, R. A. Structure-based identification of binding sites, native ligands and potential inhibitors for G-protein coupled receptors. *Proteins* **2003**, *51*, 423–433.
- (31) Cavasotto, C. N.; Ortiz, M. A.; Abagyan, R. A.; Piedrafita, F. J. In silico identification of novel EGFR inhibitors with antiproliferative activity against cancer cells. *Bioorg. Med. Chem. Lett.* **2006**, *16*, 1969–1974.
- (32) Li, B.; Duysen, E. G.; Saunders, T. L.; Lockridge, O. Production of the butyrylcholinesterase knockout mouse. *J. Mol. Neurosci.* **2006**, *30*, 193–196.
- (33) Primo-Parmo, S. L.; Bartels, C. F.; Wiersema, B.; van der Spek, A. F.; Innis, J. W.; La Du, B. N. Characterization of 12 silent alleles of the human butyrylcholinesterase (BCHE) gene. *Am. J. Hum. Genet.* **1996**, *58*, 52–64.
- (34) La Du, B. N.; Bartels, C. F.; Nogueira, C. P.; Hajra, A.; Lightstone, H.; van der Spek, A.; Lockridge, O. Phenotypic and molecular biological analysis of human butyrylcholinesterase variants. *Clin. Biochem.* **1990**, *23*, 423–431.
- (35) Wadkins, R. M.; Hyatt, J. L.; Yoon, K. J.; Morton, C. L.; Lee, R. E.; Damodaran, K.; Beroza, P.; Danks, M. K.; Potter, P. M. Identification of novel selective human intestinal carboxylesterase inhibitors for the amelioration of irinotecan-induced diarrhea: Synthesis, quantitative structure–activity relationship analysis, and biological activity. *Mol. Pharmacol.* **2004**, *65*, 1336–1343.
- (36) Wadkins, R. M.; Hyatt, J. L.; Edwards, C. C.; Tsurkan, L.; Redinbo, M. R.; Wheelock, C. E.; Jones, P. D.; Hammock, B. D.; Potter, P. M. Analysis of mammalian carboxylesterase inhibition by trifluoromethylketone-containing compounds. *Mol. Pharmacol.* **2007**, *71*, 713–723.
- (37) Lundstedt, T.; Seifert, E.; Abramo, L.; Thelin, B.; Nystrom, A.; Pettersen, J.; Bergman, B. Experimental design and optimization. *Chemom. Intell. Lab. Syst.* **1998**, *42*, 3–40.
- (38) Potter, P. M.; Wadkins, R. M. Carboxylesterases—Detoxifying enzymes and targets for drug therapy. *Curr. Med. Chem.* **2006**, *13*, 1045–1054.
- (39) Bencharit, S.; Morton, C. L.; Howard-Williams, E. L.; Danks, M. K.; Potter, P. M.; Redinbo, M. R. Structural insights into CPT-11 activation by mammalian carboxylesterases. *Nat. Struct. Biol.* **2002**, *9*, 337–342.
- (40) Bencharit, S.; Morton, C. L.; Xue, Y.; Potter, P. M.; Redinbo, M. R. Structural basis of heroin and cocaine metabolism by a promiscuous human drug-processing enzyme. *Nat. Struct. Biol.* **2003**, *10*, 349–356.
- (41) Medvedev, A. E.; Ivanov, A. S.; Kamysanskaya, N. S.; Kirkel, A. Z.; Moskvitina, T. A.; Gorkin, V. Z.; Li, N. Y.; Marshakov, V. Interaction of indole derivatives with monoamine oxidase A and B. Studies on the structure-inhibitory activity relationship. *Biochem. Mol. Biol. Int.* **1995**, *36*, 113–122.
- (42) Chapman, J. G.; Magee, W. P.; Stukenbrok, H. A.; Beckius, G. E.; Milici, A. J.; Tracey, W. R. A novel nonpeptidic caspase-3/7 inhibitor, (S)-(+)-5-[1-(2-methoxymethylpyrrolidinyl)sulfonyl]isatin reduces myocardial ischemic injury. *Eur. J. Pharmacol.* **2002**, *456*, 59–68.
- (43) Lee, D.; Long, S. A.; Adams, J. L.; Chan, G.; Vaidya, K. S.; Francis, T. A.; Kikly, K.; Winkler, J. D.; Sung, C. M.; Debouck, C.; Richardson, S.; Levy, M. A.; DeWolf, W. E. Jr.; Keller, P. M.; Tomaszek, T.; Head, M. S.; Ryan, M. D.; Haltiwanger, R. C.; Liang, P. H.; Janson, C. A.; McDevitt, P. J.; Johanson, K.; Concha, N. O.; Chan, W.; Abdel-Meguid, S. S.; Badger, A. M.; Lark, M. W.; Nadeau, D. P.; Suva, L. J.; Gowen, M.; Nuttall, M. E. Potent and selective nonpeptide inhibitors of caspases 3 and 7 inhibit apoptosis and maintain cell functionality. *J. Biol. Chem.* **2000**, *275*, 16007–16014.
- (44) Lee, D.; Long, S. A.; Murray, J. H.; Adams, J. L.; Nuttall, M. E.; Nadeau, D. P.; Kikly, K.; Winkler, J. D.; Sung, C. M.; Ryan, M. D.; Levy, M. A.; Keller, P. M.; DeWolf, W. E., Jr. Potent and selective nonpeptide inhibitors of caspases 3 and 7. *J. Med. Chem.* **2001**, *44*, 2015–2026.
- (45) Merritt, E. A.; Bacon, D. J. Raster 3D: Photorealistic molecular graphics. *Methods Enzymol.* **1997**, *277*, 505–524.
- (46) Kraulis, P. J. MOLSCRIPT: A program to produce both detailed and schematic plots of protein structures. *J. Appl. Crystallogr.* **1991**, *24*, 946–950.

JM061471K